Dielectric and piezoelectric properties of $Ba(Zr_xTi_{1-x})O_3$ lead-free ceramics

Wei Li,* Zhijun Xu, Ruiqing Chu, Peng Fu, and Guozhong Zang
College of Materials Science and Engineering, PlaceNameLiaocheng PlaceTypeUniversity, Liaocheng 252059, country-regionplaceChina
(Received on 19 May, 2010)

Lead-free ceramics $Ba(Zr_xTi_{1-x})O_3$ $(x = 0.02-0.2)$ were prepared using a solid-state reaction technique. The structural and electrical properties were systemically investigated. Crystalline structures and microstructures were analyzed by X-ray diffraction and scanning electron microscope (SEM) at room temperature. All the samples possess pure perovskite structure. A small amount of Zr content has great effect on the microstructure of $Ba(Zr_xTi_{1-x})O_3$ ceramics. The homogeneous microstructure with grain size about 30μm is obtained for the sample at $x = 0.05$. The phase transitions merge together in one peak for the samples at $x = 0.10$ and the highest dielectric constant 15900 is obtained for the sample at $x = 0.15$. The $Ba(Zr_xTi_{1-x})O_3$ ceramics at x=0.05 exhibit excellent piezoelectric properties of high $d_{33} = 208\ pC/N$, $k_p = 31.5\%$ and $Q_m = 500$.

Keywords: Ceramics; Microstructure; Dielectric properties; Piezoelectric properties.

1. INTRODUCTION

Lead zirconate titanate (PZT) ceramics are the most widely used piezoelectric materials due to their superior piezoelectric properties close to the morphotropic phase boundary (MPB) between rhombohedral and tetragonal phases. Nevertheless, they are not environment friendly for lead oxide toxicity. With the recent growing demand of global environmental protection, many researchers have greatly focused on lead-free ceramics to replace the lead-based ceramics [1-3].

Barium titanate ($BaTiO_3$) is one of the most widely studied lead-free piezoelectric material [4-10]. It is well known that $BaTiO_3$, which is a typical ABO_3 perovskite-type material, has five kinds of crystal systems: hexagonal, cubic, tetragonal, orthorhombic and rhombohedral, depending on the phase transition temperature: 1432 ^0C, 130 ^0C, 5 ^0C and -90 ^0C, respectively [5,6]. Donor-doping $BaTiO_3$ solid solutions with ions (e.g., Ca^{2+}, Sr^{2+}, La^{3+}, Zr^{4+} and Nb^{5+}, etc.) have been and continue to be of interest for investigation, not only because of their various applications, but also for their interesting dielectric and ferroelectric behaviors [7-9]. In particular, compositionally modified $BaZr_xTi_{1-x}O_3$ (BZT) receives much attention due to the tunable structure and electrical properties to specific applications, because of Zr^{4+} is chemically more stable than Ti^{4+} [9]. The polymorphic phase transitions of $BaZr_xTi_{1-x}O_3$ (rhombohedral – orthorhombic T_1, orthorhombic – tetragonal T_2 and tetragonal – cubic T_c) move closer with increasing Zr content and merge near room temperature for the composition of $x = 0.15$. Further increase in Zr content, especially for $x >$ 0.25, the samples show broad dielectric peaks with frequency dispersion, i.e., ferroelectric-relaxor behavior [10,11]. In the last few years, BZT ceramics have been used as a dielectric material in multi-layer ceramic capacitors (MLCC). The compositional and microstructure modification play important roles to meet the required dielectric constant and dielectric temperature characteristic, however, dependence of ferroelectric properties on Zr content has not been well understand [12,13]. In this work, the structure, dielectric properties and ferroelectric properties of the $BaZr_xTi_{1-x}O_3$ $(x = 0.02-0.2)$ ceramics as a function of Zr content were systemically investigated.

2. EXPERIMENTAL

$BaZr_xTi_{1-x}O_3$ ceramics of x=0.02, 0.05, 0.07, 0.10, 0.15 and 0.20 were prepared by conventional solid-state reaction technique, respectively. Raw materials of $BaCO_3$ (99.0%), ZrO_2 (99.0%) and TiO_2 (99.5%) were mixed with addition of alcohol, then dried and calcined at 1200 ^{0}C for 4 h. Thereafter, they were remixed and pressed into 12mm-diam pellets and sintered at 1400 ^{0}C for 5 h in air. The sample crystallization behavior was examined using an X-ray diffraction meter using a Cu K_α radiation (λ =1.54178 Å) (XRD, D8 Advance, Bruker Inc., Germany). The dielectric properties were measured by the precision impedance analyzer (4294 Agilent Inc., America) controlled by a computer at 100kHz with the testing temperature ranged from room temperature to 200 ^{0}C. Ferroelectric hysteresis loops were measured at room temperature using an aix-ACCT TF2000FE-HV ferroelectric test unit (aix-ACCT Inc., Germany). The piezoelectric constant d_{33} was measured using a tester quasi-static d_{33} meter (YE2730 SINOCERA, China). The mechanical quality factor Q_m and the planar electromechanical coupling factor k_p were calculated following IEEE standards by using the impedance analyzer.

3. RESULTS AND DISCUSSION

Figure 1 shows the XRD patterns of the $Ba(Zr_xTi_{1-x})O_3$ ceramics. As can be seen, all the samples show pure perovskite structure, suggesting that Zr diffuse into the $BaTiO_3$ lattice to form a solid solution. Moreover, it is clearly seen that the diffraction peaks (220) at 66 ^{0} shift significantly to low angle with increasing Zr content. Although the microscopic mechanism underlying this observation is currently unclear, the obvious shift and evolution of the splitting (202)/(220) peaks with increasing Zr content imply that Zr doping not only induces the lattice distortion but also changes the phase composition of $Ba(Zr_xTi_{1-x})O_3$ ceramics. Due to the fact that the ionic radius of Zr^{4+} (0.86

*Electronic address: liwei_727@yahoo.cn

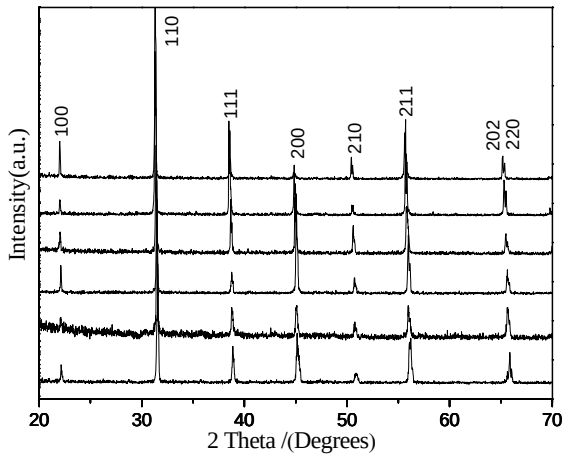

FIG. 1: X-ray diffraction patterns of the $Ba(Zr_xTi_{1-x})O_3$ ceramics at x=0.02, 0.05, 0.07, 0.10, 0.15 and 0.20.

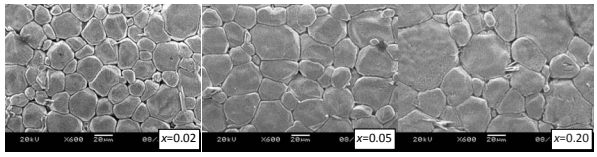

FIG. 2: SEM micrographs of the $Ba(Zr_xTi_{1-x})O_3$ ceramics at x=0.02, 0.05 and 0.20.

Å) is larger than that of Ti^{4+} (0.75 Å), thus, the substitution of Ti^{4+} with Zr^{4+} could increase the lattice parameter of ceramics [14,15]. Fig. 2 shows the SEM micrographs of $Ba(Zr_xTi_{1-x})O_3$ ceramics (x=0.02, 0.05 and 0.20). The microstructure of $Ba(Zr_{0.02}Ti_{0.98})O_3$ ceramics is inhomogeneous and some distinct pores exist in the grain boundary. For the sample at x=0.05, the microstructure is homogeneous and little pores exist in the grain boundary, while the grain size is about 30μm. It is well known that clear grain boundary and uniformly distributed grain size could enhance the mechanical strength of piezoelectric ceramics and be advantageous to the electric properties [16]. For the sample at x=0.20, the microstructure is inhomogeneous and some of the grain size become singularly large (50μm).

The dielectric constants as a function of temperature for the $Ba(Zr_xTi_{1-x})O_3$ system measured at frequency of 100 kHz are shown in Fig. 3. As can be seen, two obvious phase transitions above 20^0C corresponding to the orthorhombic-tetragonal and tetragonal-cubic, respectively, are observed for the samples of x=0.02-0.07. The T_c shifts to lower temperature while T_2 shifts to higher temperature with the increase of Zr content. This is the well-known pinching effect in these compositions [10]. With further increase of Zr content, at x =0.10, the three phase transitions merge together in one broad peak. This result is different from the previous studies, i.e., the three phase transitions merge together at x=0.15 [13]. On the other hand, the dielectric constants of $Ba(Zr_xTi_{1-x})O_3$ ceramics increase with increasing Zr content. The highest dielectric constant (15900) is obtained for the sample at x =0.15.

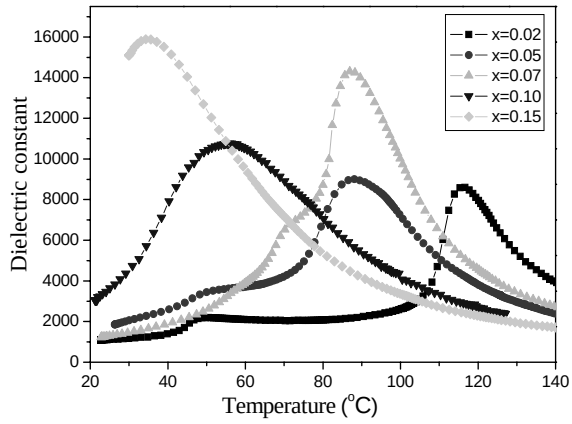

FIG. 3: Temperature dependence of dielectric constant for the $Ba(Zr_xTi_{1-x})O_3$ ceramics at x =0.02, 0.05, 0.07, 0.10, 0.15 and 0.20 measured at 100 kHz.

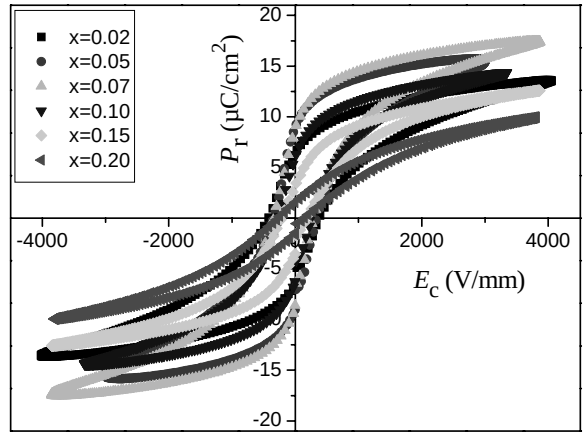

FIG. 4: Polarization vs electric field for various Zr content samples at room temperature.

The hysteresis loops of polarization versus electric field are shown in Fig. 4. The remnant polarization P_r and the coercive fields E_c as a function of composition are shown in Fig. 5. It can be seen that the coercive field of the $Ba(Zr_xTi_{1-x})O_3$ ceramics at x =0.02 is 390V/mm, while the value decreases continuously with the increase of Zr content. The coercive fields of the $Ba(Zr_xTi_{1-x})O_3$ ceramics at x =0.05, x =0.07, x =0.10, x =0.15 and x =0.20 are 330V/mm, 260V/mm, 240V/mm, 180V/mm, and 140V/mm, respectively. With increasing Zr content, the remnant polarizations of the $Ba(Zr_xTi_{1-x})O_3$ ceramics increase to a maximum value 9.0 $\mu C/cm^2$ at x=0.05 and then decrease. Fig. 6 shows the piezoelectric coefficient d_{33}, planar mode electromechanical coupling coefficient k_p and mechanical quality factor Q_m of $Ba(Zr_xTi_{1-x})O_3$ ceramics as a function of Zr content. At x=0.02, d_{33}, k_p and Q_m are 198 pC/N, 28.8% and 210, respectively. With raising of x to 0.05, the d_{33}, k_p

and Q_m reach their maximum values of 208 pC/N, 31.5% and 500, respectively. The highest d_{33} value 208 pC/N of the $Ba(Zr_xTi_{1-x})O_3$ ceramics could be attributed to the relative high P_r ($9.0\ \mu C/cm^2$) and low $E_c(330V/mm)$ for the sample at x=0.05. The highest Q_m (500) for the sample at x =0.05, which is twice as large as other $Ba(Zr_xTi_{1-x})O_3$ ceramic, is considered to be reasonably consistent with it's clear grain boundary and uniformly distributed grain size.

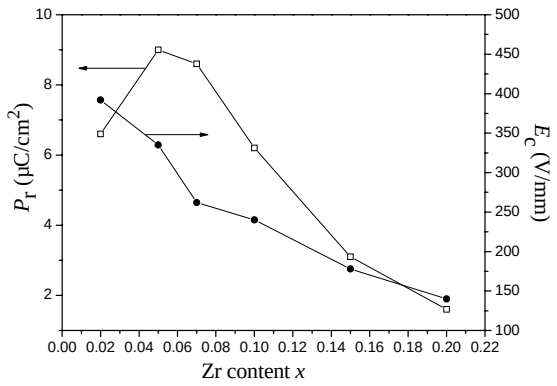

FIG. 5: P_r and E_c variations with x of the $Ba(Zr_xTi_{1-x})O_3$ ceramics.

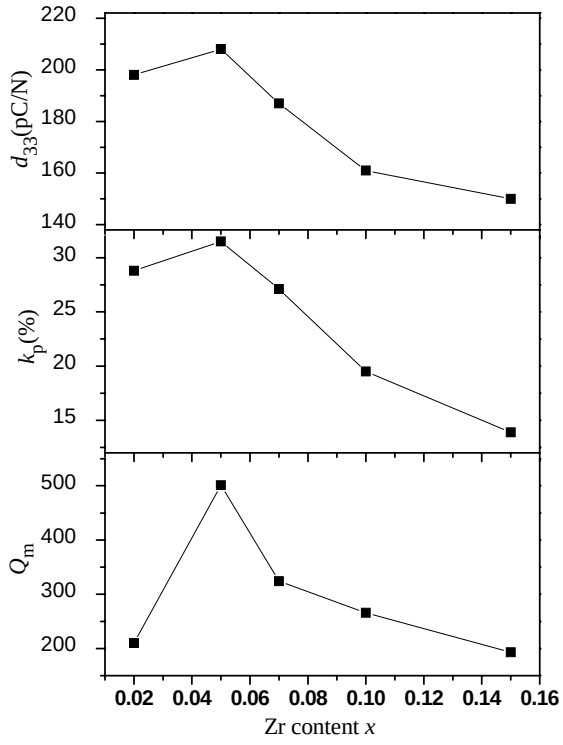

FIG. 6: Piezoelectric constant d_{33}, planar electromechanical coefficient k_p and mechanical quality factor Q_m of the $Ba(Zr_xTi_{1-x})O_3$ ceramics as a function of x.

4. CONCLUSIONS

Lead-free $Ba(Zr_xTi_{1-x})O_3$ (x =0.02-0.2) ceramics prepared by solid-state reaction were systemically investigated. Results show that all the samples are pure perovskite structure. The phase transitions merge together for the samples at x =0.10 and the highest dielectric constant 15900 is obtained for the sample at x =0.15. The ceramics at x =0.05 exhibite excellent piezoelectric properties of high d_{33} = 208 pC/N, k_p =31.5% and Q_m=501.

Acknowledgments

This work was supported by the program for the National Natural Science Foundation of China (Grant No. 50602021 and Grant No. 50802038) and Research Foundation of Liaocheng University (No. X0810041).

[1] Y. Saito, H. Takao, T. Tani, T. Nonoyama, K. Takatori, T. Homma, T. Nagaya, and M. Nakamura, Nature **432** 84 (2004).
[2] E. Hollenstein, M. Davis, D. Damjanovic, and N. Setter, Appl. Phys. Lett. **87** 182905 (2005).
[3] P. Kantha, K. Pengpat, P. Jarupoom, U. Intatha, G. Rujijanagul, and T. Tunkasiri, Curr. Appl. Phys. **9** 460 (2009).
[4] Z. Yu, R.Y. Guo, and A. S. Bhalla, J. Appl. Phys. **88** 410 (2000).
[5] X.S. Wang, L.L. Zhang, H.Liu, J.W. Zhai, X. Yao, Mater. Chem. Phys. **112** 675 (2008).
[6] C.J. Xiao, C.Q. Jin, X.H. Wang, Mater. Chem. Phys. **111** 209 (2008).
[7] P.Z. Zhang, M.R. Shen, L. Fang, F.G. Zheng, X.L. Wu, J.C. Shen, and H.T. Chen Appl. Phys. Lett. **92** 222908 (2008).
[8] R.L. Brutchey, G.S. Cheng, Q. Gu, and D.E. Morse, Adv. Mater. **20** 1029 (2008).
[9] T. Maiti, R. Guo, and A.S. Bhalla, Appl. Phys. Lett. **89** 122909 (2006).
[10] P.S. Dobal, A. Dixit, and R.S. Katiyar, J. Appl. Phys. **89** 8085 (2001).
[11] Z. Yu, R. Guo, A.S. Bhalla, J. Cryst. Growth **233** 460 (2001).
[12] F. Zimmermann, M. Voigts,W. Menesklou, E. Ivers-Tiffe'e, J. Eur. Ceram. Soc. **24** 1729 (2004).
[13] Z. Yu, C. Ang, R.Y. Guo, and A. S. Bhalla, J. Appl. Phys. **92** 2655 (2002).
[14] B.L. Cheng, C.Wang, S.Y.Wang, H. Lu, Y.L. Zhou, Z.H. Chen, and G.Z. Yang, J. Eur. Ceram. Soc. **25** 2295 (2005).
[15] P.Z. Zhang, M.R. Shen, L. Fang, F.G. Zheng, X.L. Wu, J.C. Shen, and H.T. Chen, Appl. Phys. Lett. **92** 222908 (2008).
[16] Z.P. Yang, B. Liu, L.L. Wei, Y.T. Hou, Mater. Res. Bull. **43** 81 (2008).